thermo

MDPI

Article

Heat Treatment Effects on β Ti-10Mo-xMn Alloys for Biomedical Applications

Mariana Luna Lourenço [1], Pedro Akira Bazaglia Kuroda [2,*] and Carlos Roberto Grandini [1]

[1] Laboratório de Anelasticidade e Biomateriais, Universidade Estadual Paulista (UNESP), Bauru 17033-360, SP, Brazil; mariana.lourenco@unesp.br (M.L.L.); carlos.r.grandini@unesp.br (C.R.G.)
[2] Instituto Latino-Americano de Ciências da Vida e da Natureza (ILACVN), Universidade Federal da Integração Latino-Americana (UNILA), Foz do Iguaçu 85870-650, PR, Brazil
* Correspondence: pedro.kuroda@ufscar.br

Abstract

When it comes to developing new titanium alloys for biomaterials, β metastable alloys have been gaining the most attention from researchers, as they have a lower elastic modulus and the microstructure can be altered by adding other elements and heat treatments (HT), which makes the material a promising biomaterial. The Ti-10Mo-Mn alloys were melted in an arc furnace. After ingot casting, a homogenization treatment (#T) was carried out, followed by the mechanical processing of hot rolling (#1) and subsequent annealing HT (#2). This work aimed to analyze the influence of some HT on the phase constituents, percentages, morphologies, distributions and selected mechanical properties, such as microhardness and elastic modulus in Ti-10Mo-xMn system alloys, ranging from 0 to 8% by weight. The results showed that alloys with low manganese content, classified as metastable, were sensitive to the HT in this study. From 4% manganese, the alloys had a stable β phase and were, therefore, not sensitive to the HT. The hardness of the alloys with 0 and 2% manganese remained high, possibly due to the presence of the omega phase. The elastic modulus increased from the hot rolling condition (#1) to annealing condition (#2) in all compositions. The Ti-10Mo-2Mn#1 alloy stood out among the alloys studied. It showed the lowest elastic modulus (~87 GPa), making it suitable for use as a biomaterial.

Keywords: titanium alloys; beta metastable; heat treatment; biomaterial

check for updates

Academic Editor: Johan Jacquemin

Received: 19 September 2025
Revised: 29 October 2025
Accepted: 30 October 2025
Published: 3 November 2025

Citation: Lourenço, M.L.; Kuroda, P.A.B.; Grandini, C.R. Heat Treatment Effects on β Ti-10Mo-xMn Alloys for Biomedical Applications. *Thermo* **2025**, *5*, 46. https://doi.org/10.3390/thermo5040046

Copyright: © 2025 by the authors. Licensee MDPI, Basel, Switzerland. This article is an open access article distributed under the terms and conditions of the Creative Commons Attribution (CC BY) license (https://creativecommons.org/licenses/by/4.0/).

1. Introduction

Titanium alloys are widely used in various fields, including biomedicine, due to their excellent properties, high corrosion resistance, fatigue resistance, and excellent biocompatibility. Although the Ti-6Al-4V alloy is predominant, the release of Al and V ions is a long-term concern, driving research into safer compositions. Among the different types of titanium alloys, β-type alloys have gained prominence due to their ability to have a low modulus of elasticity, close to that of human bones, which minimizes the stress shielding effect and presents better osseointegration [1]. To stabilize this phase, elements such as Mo and Mn are investigated. Mo is recognized for its high capacity to stabilize the β phase and increase the strength of the alloy. Mn, on the other hand, is a biocompatible element, essential for bone development, and low cost, which makes it an economical alternative. Previous studies, such as that by Santos et al., have already validated the potential of the synergistic combination of these elements, showing that the addition of Mo to Ti-Mn alloys significantly improves ductility without compromising mechanical strength, making the Ti-Mo-Mn system a promising field for the development of new implants.

Beta titanium alloys are well-known for their excellent combination of mechanical properties, corrosion resistance, and biocompatibility, making them highly suitable for biomedical applications. However, conventional beta-Ti alloys often depend on expensive beta-stabilizing elements such as tantalum (Ta), molybdenum (Mo), and niobium (Nb), which significantly increase production costs. As an alternative, researchers have explored the addition of manganese (Mn) due to its relatively low cost and effective beta-stabilizing properties. Incorporating Mn into titanium-based alloys presents a promising approach to reduce material costs while preserving the favorable mechanical and structural characteristics of β-Ti alloys, thereby making them more accessible for widespread use in biomedical fields.

The elastic modulus of a titanium alloy is strongly influenced by its microstructure, which in turn can be modified by heat treatment. When subjected to suitable heat treatments, the metastable β phase can be decomposed into different microstructures, each with different mechanical properties [2].

The selection of the heat treatment and its parameters, such as temperature, time, and cooling rate, is crucial in controlling the precipitation of phases and grain size, directly influencing the mechanical properties of the alloy. For example, rapid water cooling can lead to martensite formation, resulting in greater hardness. In contrast, slow furnace cooling can favor the formation of a lamellar microstructure with greater fracture toughness [2].

Understanding the relationship between heat treatments and the resulting microstructure and mechanical properties is essential for developing metastable β titanium alloys with optimized performance for biomedical applications [2].

Heat treatment involves heating the material to a predefined temperature for a specific period, followed by a controlled cooling process to achieve the desired properties. This process manages to alter the microstructure of the material, so the mechanical properties dependent on the microstructure are also altered [3,4].

Gupta et al. [5] studied the evolution of the microstructure of the Ti-15V-3Cr-3Al-3Sn alloy during aging heat treatments for up to 6 h from 450 °C to 700 °C. The results showed that the supersaturated β phase obtained after solution treatment at 800 °C gives way to the more stable α phase and that the fraction of the α phase increases with temperature. Increasing the aging temperature and prolonging the duration results in the formation of α-phase precipitates at the grain boundaries and within the grains themselves.

Xavier et al. [6] analyzed the influence of heat treatment on the microhardness and microstructure of Ti-15Zr-xMo alloys. This process led to an increase in the amount of α' phase, which significantly reduced the alloy's microhardness.

Kuroda et al. [7] studied solubilization heat treatment times in alloys of the Ti-25Ta-xZr system, the treatment was at 1000 °C with a heating rate of 10 °C/min, keeping it at this temperature for 0, 3, and 6 h with water quenching. The α-type alloys had fine needles inside the grains, and their grain boundaries were related to the structures of the α phase; with increasing time in the treatments, there was a decrease in these structures, indicating greater stability of the β phase.

This paper aimed to analyze the influence of some heat treatments on the structure, microstructure, microhardness, and elastic modulus of Ti-10Mo-xMn ternary alloys, varying the manganese content between 0 and 8% by weight.

2. Materials and Methods

The Ti-10Mo-xMn alloys (x = 0, 2, 4, 6, and 8% by weight) were melted in an arc furnace, and all initial characterization was described in detail in the work of Lourenço and collaborators [8].

In this work, the Ti-10Mo-xMn was used by different thermomechanical treatments (HT) to alter the crystalline phases and, consequently, change the value of the elastic modulus. The first was homogenization heat treatment (#T), which relieved the internal stresses in the ingots produced in the arc furnace [9]. These stresses come from the crucible's cooling gradient during the melting process. The homogenization treatment was performed in a steel tube with an isolated system and vacuum conditions of 10–5 Torr, followed by a heating rate of 10 °C/min, reaching a temperature of 1000 °C and remaining at this temperature for 24 h [10]. The ingot was cooled slowly at 10 °C/min so that the homogenized bonds remained in thermodynamic equilibrium.

After HT (#T), hot rolling was carried out (#1), which is heating the material and passing the ingot between two rolling rolls to reduce the material's thickness and obtain an ingot with a regular shape. The ingots, with a thickness of approximately 20 mm, were heated to approximately 1000 °C and passed through the rolling rolls; with each step, a thickness of 1.0 mm was decreased. At each rolling step, the ingots were put back into the muffle furnace to ensure that the whole mechanical forming process was carried out at a temperature of 1000 °C. Blades with approximately 4.0 mm thickness were obtained.

An oxidation layer was created on the ingots that were removed with a manual sanding process and a chemical attack with acid solution (HNO_3 50% and HF 50%) until they reached a silver color again, observing that the oxidation was completely removed.

The annealing HT (#2) was carried out after the rolling process to relieve internal stresses and remove the imperfections in the microstructure caused by mechanical processing, which alter the material's mechanical properties. This HT (#2) was performed in a steel tube in 10^{-5} Torr vacuum, with a heating rate of 10 °C/min, up to 1000 °C, and remaining at this temperature for 6 h, with slow cooling at 10 °C/min, until reaching room temperature [11,12].

Figure 1 shows a diagram of the thermomechanical processes performed in this work.

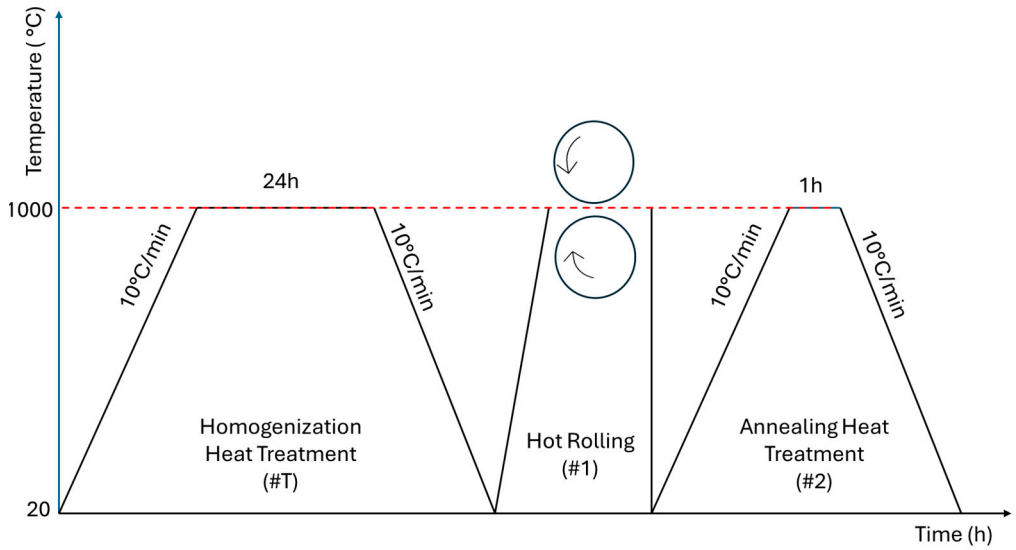


Figure 1. Diagram of the thermomechanical processes performed on the samples after melting.

After each processing, the samples were characterized. X-ray measurements were performed using Rigaku equipment, model D/max-2100 PC (Akishima City, Tokyo, Japan). The radiation was Cu-Kα, with wavelength λ = 1.544 Å, current of 20 mA, and potential of 40 kV. The measurements were performed in fixed-time mode, with a step of 0.02°, ranging from 30° to 80°, and a residence time of 1.6 s.

The diffraction patterns of the X-ray waves were simulated using the Rietveld method. The percentage of crystalline phases present in the produced materials, the lattice parameter

and the phase constitute were quantified from the Rietveld. The GSAS 1 program with EXPGUI interface was refined using Ti crystallographic files from the ICSD (Inorganic Crystal Structure Database) database [13,14]. The lattice parameters were calculated directly by the Rietveld program during the refinement process, based on the peak positions of the diffraction patterns using Bragg's law and the corresponding Miller indices (hkl).

The microstructure of the metals was analyzed using optical microscopy techniques, an Olympus BX51M model optical microscope (OM; BX51M microscope, Olympus Ltd., Westborough, MA, USA), and scanning electron microscopy, SEM, and EVO LS15 models from Carl Zeiss (SEM, Carl Zeiss, Oberkochen, Germany). To obtain the micrographs, the alloys underwent standard metallographic preparation, which included grinding with silicon carbide papers from 300 to 1500 mesh, polishing with 1 μm alumina, and chemical etching using Kroll's reagent, as described by Kuroda [15].

Hardness and elastic modulus measurements were performed to verify the influence of heat treatments on the mechanical properties of Ti-Mo-Mn alloys. The Shimadzu HMV-2 (Shimadzu, Barueri, Brazil) microhardness meter was used for this measurement and connected to a computer. The configuration used was a load of 1.961 N for 60 s for each indentation [16,17]. The impulse excitation technique (ASTM, 2002 #1427) with the Sonelastic® equipment from ATCP (ATCP Physical Engineering, São Carlos, Brazil) was utilized for the elastic modulus measurements [18–21].

Table 1 presents the nomenclature established for the processing conditions. It is recalled that the term #T refers to homogenization heat treatment, #1 to the hot rolling process, and #2 to annealing heat treatment (stress relief).

Table 1. Corresponding symbols for each material processing status.

Symbol	Condition
#T	Heat treatment homogenization
#1	Hot rolling
#2	Heat treatment annealing

3. Results and Discussion

3.1. X-Ray Results

Figure 2 presents the X-ray diffractograms of the Ti-10Mo (0Mn), Ti-10Mo-2Mn, Ti-10Mo-4Mn, Ti-10Mo-6Mn, and Ti-10Mo-8Mn alloys, varying the processing conditions.

The XRD graphs presented in Figure 1 show the β-stabilizer character of manganese, where the addition of this element in the alloy promoted the formation of the β phase and suppression of the α and α″ doses. In condition #T, peaks of phases β and α were observed in the Ti-10Mo (0Mn) and Ti-10Mo-2Mn alloys. In contrast, in condition #1, there was a decrease in the diffraction peaks of the martensitic phases, indicating an increase in the amount of β phase in the alloys when submitted to the hot rolling process. Rolling can be considered a rapid cooling, due to the enormous temperature gradient between the alloy heated to 1000 °C and the metal rolling rolls. There is β retention and transformation from the α to α″ phase ($\alpha \rightarrow \alpha''$) because the mechanical forming of hot rolling conditions the alloys to retain the high-temperature phases.

The literature shows that rolling can retain the α″ phase in β-metastable titanium alloys, as shown by Hanada et al. [22] and Nunes et al. [23]. It is important to note that the studies reporting this phenomenon carried out the cold rolling process, where the heating parameter is not included as a thermodynamic condition. In this work, as the rolling was performed hotly to facilitate mechanical forming, there is also a greater probability of β phase retention.

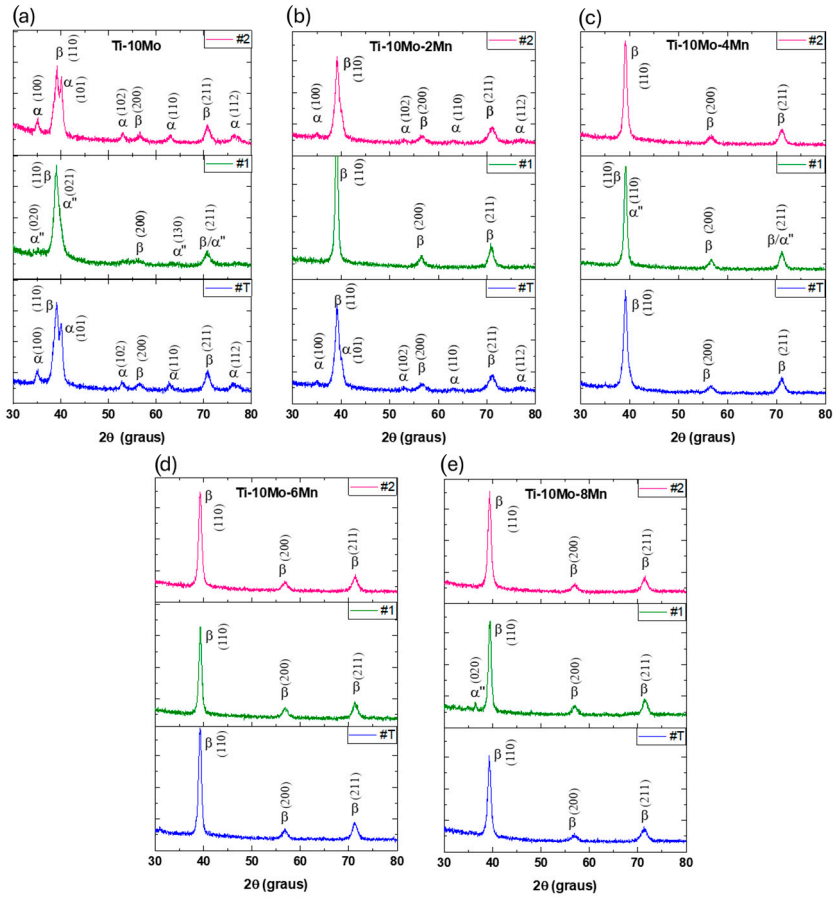


Figure 2. X-ray diffractograms of the homogenized, rolled and annealed samples (**a**) Ti-10Mo (0Mn); (**b**) Ti-10Mo-2Mn; (**c**) Ti-10Mo-4Mn; (**d**) Ti-10Mo-6Mn; (**e**) Ti-10Mo-8Mn.

Kuroda and collaborators also observed the formation of the α'' phase in α detention after a heat treatment followed by rapid cooling. In Ti alloys, when a heat treatment is performed with rapid cooling from the β field, it can stimulate the formation of the martensite phase α'' and β. The α'' phase is formed due to the lack of time during cooling, which makes it difficult for the atoms to rearrange to form stable phases, producing distortions in the crystal structure [24,25].

Still dealing with the Ti-10Mo (0Mn) and Ti-10Mo-2Mn alloys, in condition #2, the HT removed the internal stresses from the mechanical process of hot rolling, and the cooling rate was slow and controlled, allowing the following phase transformations to occur: $\beta \rightarrow \alpha$ and $\alpha'' \rightarrow \alpha$, since the α phase is the stable phase of Ti at room temperature [25].

Regarding the other alloys (Ti-10Mo-4Mn, Ti-10Mo-6Mn, and Ti-10Mo-8Mn), the increase in Mn increases the stabilization of the β phase. Consequently, when submitted to thermomechanical treatments, the alloys are not sensitive to structural changes. According to the theory of equivalent Mo, all alloys produced in this work are classified as β, with the Ti-10Mo (0Mn) and Ti-10Mo-2Mn alloys being β-metastable alloys with Mo equivalent of 10.0 and 12.8, respectively, unveiling the reason why only these two alloys are sensitive to heat treatments. Alloys with Mn values greater than 4% by weight are classified as β stable alloys with a Mo equivalent value greater than 15 (15.7 for Ti-10Mo-4Mn, 18.5 for Ti-10Mo-6Mn and Ti-10Mo-8Mn with a value of 21.36 Mo equivalent).

3.2. Rietveld Refinement Results

The X-ray diffraction data were quantified using the Rietveld structural refinement technique. This value is the quotient of the experimental diffraction points by the theoretical

points simulated by the Rietveld refinement method. It compares the difference between the measured and calculated points, weighing this difference by the expected statistical noise in the data. Perfect refinement is when x^2 has a value of 1.00. A value significantly greater than 1 (e.g., >2.0) indicates that there are systematic errors and that the model does not describe the data well (there may be missing phases, incorrect structural parameters, etc.). All refinements presented have values close to 1.00, indicating good refinement, as presented in Table 2.

Table 2. Merit parameters of the Rietveld refinements on the samples.

x^2	Ti-10Mo	Ti-10Mo-2Mn	Ti-10Mo-4Mn	Ti-10Mo-6Mn	Ti-10Mo-8Mn
#T	1.279	1.203	1.309	1.094	1.262
#1	1.125	1.540	1.143	1.148	1.104
#2	1.337	1.278	1.226	1.174	1.147

Figure 3 shows the percentage of crystalline phases (α, α″ and β) calculated by the Rietveld method. In Ti-10Mo (0Mn) #T and #2 alloys, the β phase is present at 68%, with the α′ phase being the remaining phase (32%). In condition #1, the β phase is present at 74%, with the α′ phase at 26%. In the alloy with the addition of 2% Mn, the percentage of the β phase increases significantly to approximately 88% in #T and 77% in #2. The α′ phase decreases dramatically to 12 and 28% in #T and #2, respectively. In condition #1, the alloy is mostly β.

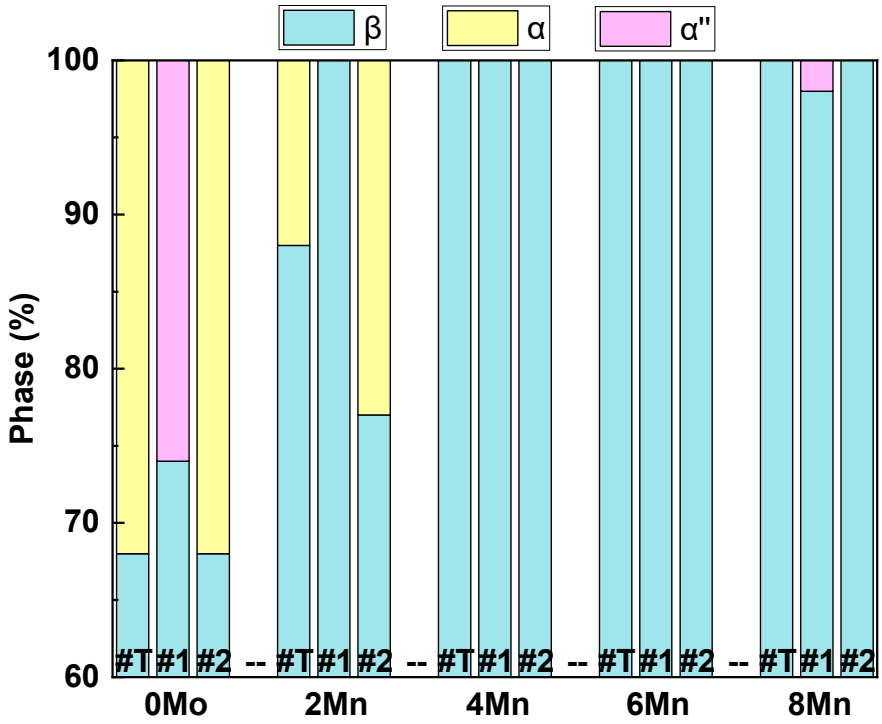


Figure 3. Percentage of crystalline phases (α, α″ and β) calculated by the Rietveld method in Ti-10Mo-xMn samples.

In the 4Mn and 6Mn alloys, the β phase is dominant in all conditions. In the 8Mn alloy in condition #1, a small fraction of the α″ phase (2%) appears, with the β phase being the largest portion (98%). In the other conditions, #T and #2, the alloys are predominantly composed of the β phase.

The results indicated that Mn acts as a β-stabilizing element, as seen in the measurements of diffraction and X-rays. In addition, it is noted that in the β-metastable alloys (Ti-10Mo (0Mn) and Ti-10Mo-2Mn), the formation of the α phase (compact hexagonal) occurs when the alloys are subjected to thermal treatment followed by slow cooling (#T and #2) and the formation of the α″ phase occurs in the lamination process. Current studies in the literature report the formation of the α″/β phases after mechanical forming performed at high temperatures and the formation of the phase β when Ti alloys are subjected to heat treatments with slow cooling [20].

It is worth noting that the α phase (HCP) has a higher atomic packing value compared to the β and α″ phases. Consequently, it is a Ti phase with a higher hardness due to the smaller interstitial volume.

3.3. Microscopic Analysis

Figure 4 shows SEM micrographs of the alloys produced in this work at a magnification of 3000×. Under homogenized sample conditions (#T), well-defined grain boundaries of the β phase are observed in all alloys, as well as small acicular structures of the α phase within the grain and the contours of the Ti-10Mo (0Mn) alloy. It is possible to observe the meeting of three grains with angles of approximately 120° between them, indicating energy stability between the adjacent contours. However, significant differences in the secondary phases are observed: while the Ti-10Mo (0Mn) alloy has small acicular structures of the α phase and grain boundaries, alloys with higher Mn contents (4Mo, 6Mo, and 8Mo) exhibit a predominantly single-phase β microstructure, with almost complete suppression of acicular precipitates. This initial observation already corroborates the role of Mn as a strong stabilizer of the β phase, expanding its stability range and inhibiting the formation of α and α″ phases in more enriched alloys. The heat treatment indicated the conditions necessary for the material to be effectively homogenized [26].

In the hot-rolled condition, micrographs reveal β-phase grain boundaries and finer acicular structures in the Ti-10Mo (0Mn) and Ti-10Mo-2Mn alloys, indicating the presence of the α martensitic phase. In alloys with higher Mn concentrations (4Mo, 6Mo, and 8Mo), the β phase remains dominant even after rolling, with the absence of secondary acicular phases, evidencing the stabilization activity of the β phase against deformation. Under these conditions, the samples were subjected to a mechanical process involving an external force, which broke the grains and left them with irregular shapes, varying sizes, and a preferential orientation in the direction of mechanical deformation, thereby increasing the internal stress in the samples [3].

In condition #2, the annealing treatment resulted in the recrystallization of the material, thereby relieving the internal stresses accumulated during rolling. In the Ti-10Mo (0Mn) and Ti-10Mo-2Mn alloys, the formation of acicular structures from the α phase is observed again. This annealing, which allows for slower cooling, favors the nucleation and growth of the α phase from the β matrix or the α″ formed during rolling, resulting in a two-phase microstructure (β + α). On the other hand, alloys with high Mn content (4Mo, 6Mo, and 8Mo) maintain an almost entirely β microstructure, indicating that Mn is sufficient to suppress phase transformations even under annealing conditions. These detailed microstructural observations are in excellent agreement with the quantitative X-ray diffraction results presented in Figure 1, which demonstrate the variation in the volumetric fractions of the α, α″ and β phases as a function of Mn content and processing, confirming the effectiveness of Mn as a β phase stabilizing element and the influence of thermomechanical treatments on the formation of secondary phases [3].

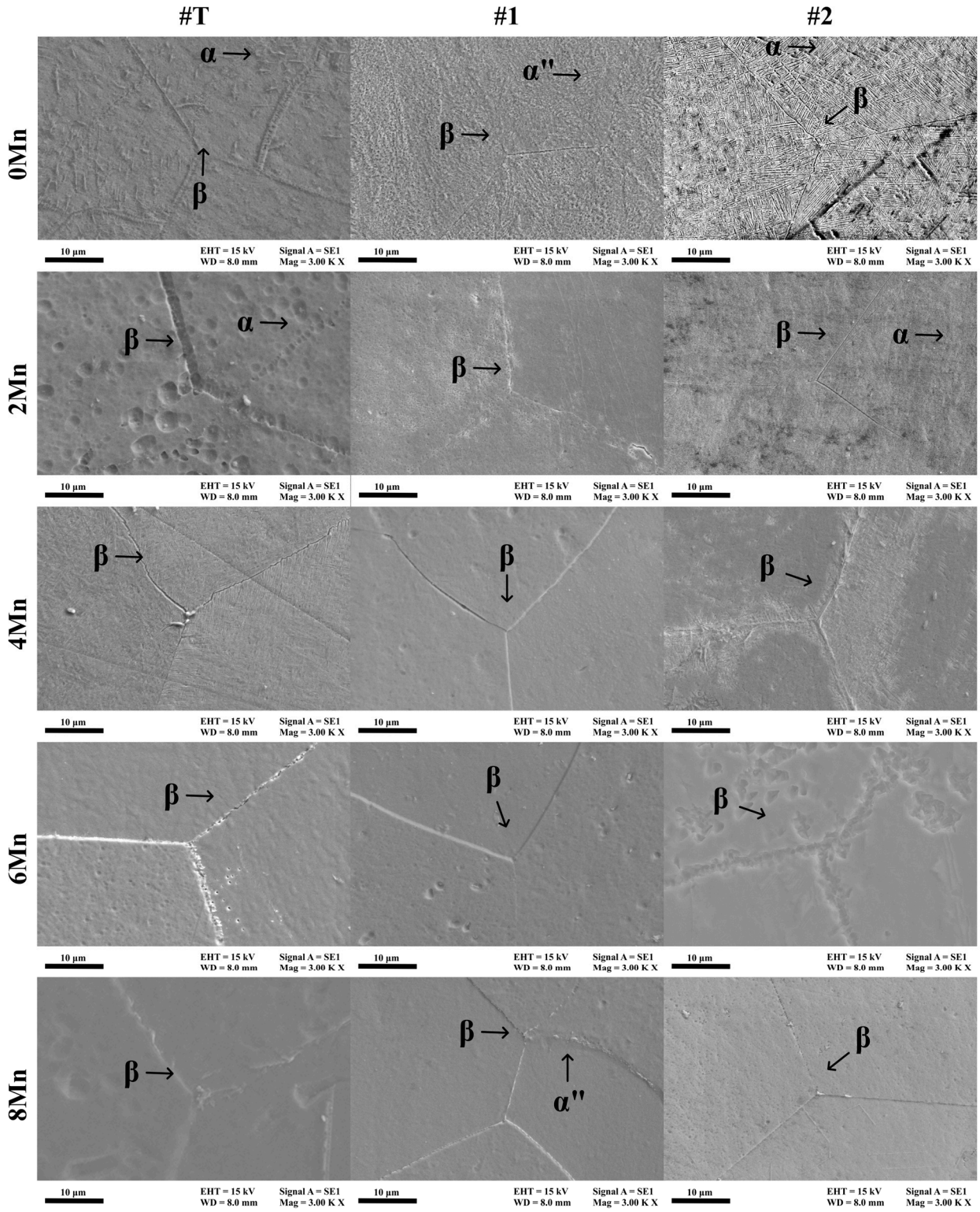


Figure 4. SEM of the alloys produced in this work at 3000× magnification.

3.4. Vickers Hardness

Biomedical materials must have hardness values that are appropriate for their application. If they have high values about the implanted tissue, it can cause wear and tear on human tissue. Another important point in the hardness study is that the material must be easily handled and molded into the necessary geometry. With high hardness values, this material becomes hard and brittle, making it difficult to manufacture implants [25].

Figure 5 illustrates the microhardness of Ti-10Mo-xMn alloys under different processing conditions, revealing a strong dependence on both Mn content and thermomechanical treatments. The metastable β alloys, Ti-10Mo (0Mn) and Ti-10Mo-2Mn (2Mn), exhibited the highest microhardness values.

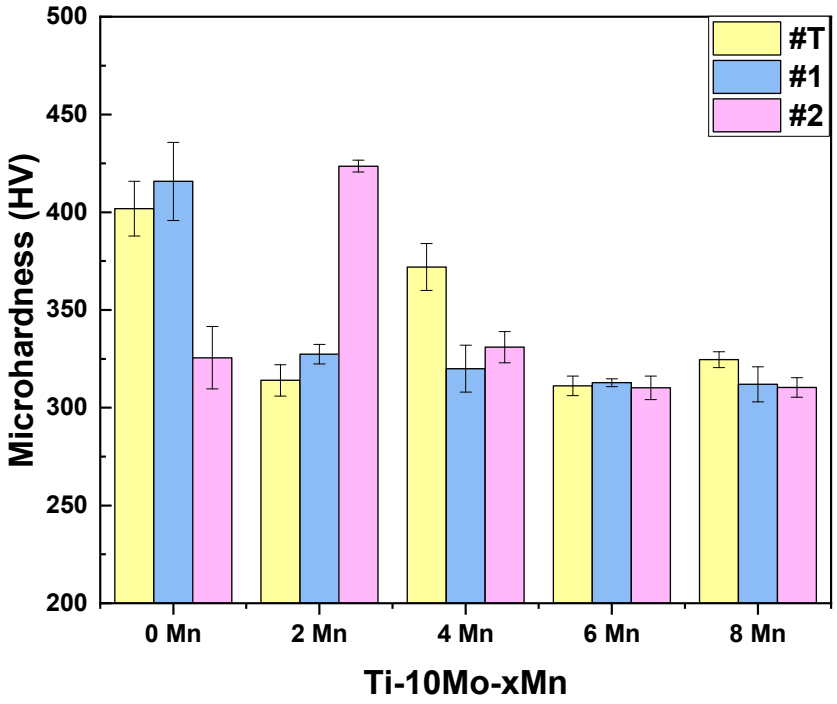


Figure 5. Hardness for Ti-10Mo-xMn alloys under conditions #T, #1, and #2 under all processing conditions.

In the Ti-10Mo (0Mn) alloy, homogenization (#T) and hot rolling (#1) conditions exhibited hardnesses around 400–415 HV, with a reduction to approximately 325 HV after annealing (#2), attributed to internal stress relief. The Ti-10Mo-2Mn alloy showed distinct behavior: starting from ~315 HV in condition #T, a slight increase in #1 (~325 HV), and a significant jump to ~425 HV in condition #2. This hardness peak is correlated with a substantial increase in the volumetric fraction of the α phase (23%) in this condition, almost double that of condition #T [11,25].

The explanation for the high hardness values in β-metastable alloys (0Mn and 2Mn) is consistently supported by the Orowan mechanism. As demonstrated by X-ray diffraction (Figure 2) and SEM micrographs (Figure 3), the presence of secondary phases (α and α″) dispersed in the β matrix acts as non-shearable precipitates. When dislocations move through the β matrix, they are forced to bypass these precipitates, generating dislocation rings and increasing resistance to plastic deformation. The possible formation of the nanometric ω phase, the hardest titanium phase, further contributes to Orowan hardening in these alloys, justifying their microhardness values superior to those of commercial biomaterials such as Ti-6Al-4V (289 HV) and CP-Ti (167 HV) [20]. The hardening observed in the Ti-10Mo-2Mn alloy in condition #2 is an excellent example of optimizing this mechanism, where the largest fraction of the α phase effectively precipitates as barriers to dislocations.

In contrast, alloys with higher manganese contents (Ti-10Mo-4Mn, Ti-10Mo-6Mn, and Ti-10Mo-8Mn) consistently exhibited lower microhardness values (approximately 300–370 HV) and were significantly less sensitive to thermomechanical treatments. This insensitivity is a direct consequence of their classification as β-stable alloys, where manganese suppresses the formation of secondary phases (α, α″, and ω). The absence of effective precipitates inhibits the Orowan hardening mechanism, resulting in a predominantly β microstructure (Figure 3) and, consequently, lower hardness. This observation reinforces

the inverse relationship between the percentage of the β phase and the hardness value, as highlighted by Kuroda et al. [7] The overall hardness of alloys in terms of phases aligns with the configuration: β + α″ + (ω) > β + α > β, underscoring the critical role of microstructure and secondary phases in controlling the mechanical properties of these alloys for biomedical applications.

3.5. Elastic Modulus

Hooke's law is the relationship between the distance between atoms and the elastic modulus. According to this law, the elastic modulus of a material is related to its stiffness and the average distance between its atoms [27]. The higher the elastic modulus, the lower the elastic deformation the material will undergo [3]. Figure 6 shows the elastic modulus of the alloys in conditions #1 and #2. The elastic modulus was not calculated in the #T condition due to the inadequacy of its geometry. For this analysis, the sample must have a regular shape with parallel faces.

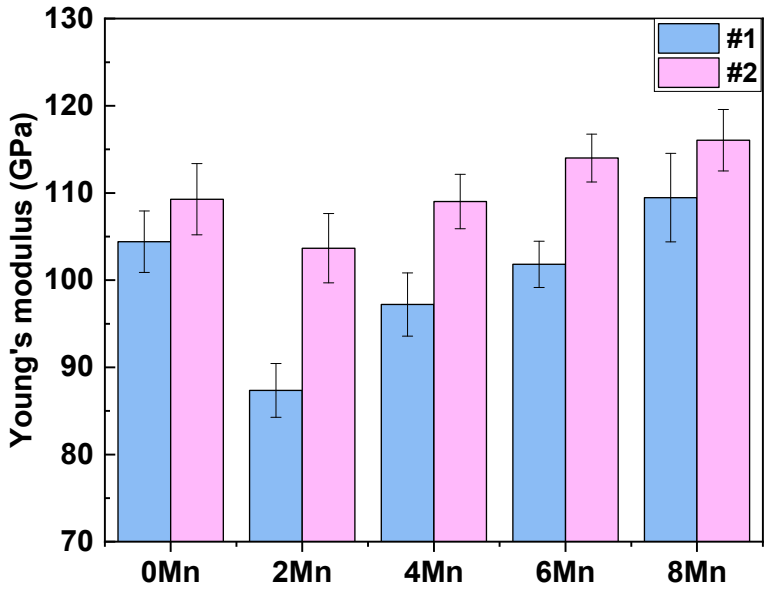


Figure 6. Elastic modulus for Ti-10Mo-xMn alloys, varying processing conditions.

It is observed that in all concentrations, the modulus increased from condition #1 to #2. Analyzing the β lattice parameters presented in Figure 7, the two processing conditions show a decrease in their value. With the lattice parameter decreasing, there is an increase in atomic binding energy, causing the elastic modulus to be increased. Therefore, it is concluded that the elastic modulus is inversely proportional to the lattice parameters.

For all Mn concentrations, the hot-rolled condition has a higher amount of β phase than the annealed condition. It is known in the literature that in Ti alloys, the phase that has the highest elastic modulus is the ω, followed by phases α, α′, α″, and finally, with a lower modulus, phase β [25]. The Ti-10Mo-2Mn alloys after hot-rolling presented an approximate modulus value of 87 GPa, the lowest value among the alloys studied, being suitable for use as a biomaterial.

Making a quick comparison, the alloys studied had an elastic modulus lower than that of the materials already used as biomaterials, Ti-6Al-4V (110 GPa), Co-Cr alloy (240 GPa), stainless steel (210 GPa) [28]. The biomaterial's elastic modulus must be close to that of human bone (30 GPa) to avoid the stress-shielding effect. The Ti-10Mo-2Mn #1 alloy had the lowest modulus among the alloys produced, approximately 87 GPa.

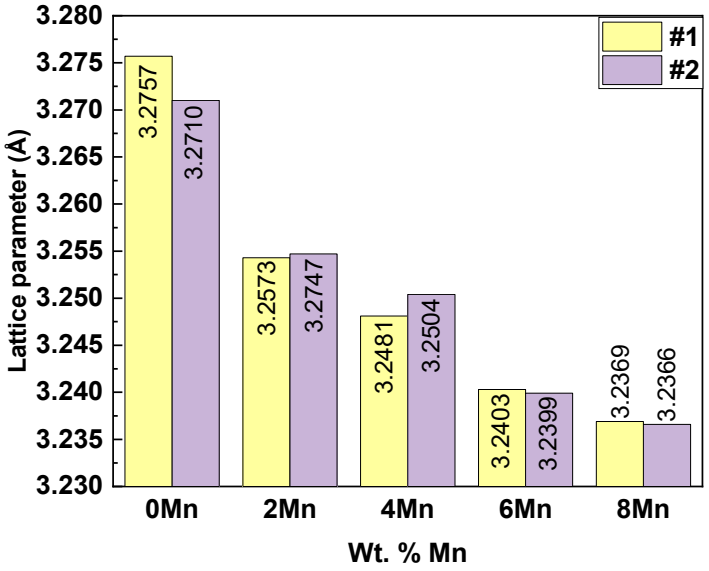


Figure 7. Phase β network parameter for Ti-10Mo-xMn alloys in the hot-rolled and annealed conditions.

4. Conclusions

Manganese is a β-stabilizing element. As it was added to the alloy, the formation of the β phase occurred, along with the suppression of the α and α″ phases. From 4% of manganese, the alloys had the β phase stabilized. Not letting the samples be sensitive to the heat treatments performed in this study.

The Ti-10Mo (0Mn) and Ti-10Mo-2Mn alloys, classified as β-metastable alloys, were sensitive to HT, changing the microstructures. From condition #T to #1, it was observed that there was an increase in the amount of phase β and the transformation of $\alpha \rightarrow \alpha''$. And from the #T conditions to #2, there was a change of $\beta \rightarrow \alpha$ and $\alpha'' \rightarrow \alpha$ since the cooling rate was slow and controlled since phase α is the stable phase of titanium at room temperature.

The hardness of Ti-10Mo (0Mn) and Ti-10Mo-2Mn alloys was high, possibly due to the undesirable presence of the ω phase. Only these two alloys had variation in the values of this property about HT; the others with 4Mn, 6Mn, and 8Mn were not sensitive to HT. The overall hardness of the alloys in terms of phases was as follows: $\beta + \alpha'' + (\omega) > \beta + \alpha > \beta$.

From condition #1 to condition #2, there was a decrease in the lattice parameter of the alloys, causing the elastic modulus to increase. It is concluded that the elastic modulus is inversely proportional to the lattice parameter. The Ti-10Mo-2Mn #1 alloy presented an approximate modulus value of 87 GPa, the lowest value among the alloys studied, being suitable for use as a biomaterial.

Author Contributions: M.L.L.: Data curation, formal analysis/interpretation, and writing—original draft. P.A.B.K.: Data curation and investigation. C.R.G.: Funding acquisition, supervision, and writing—review and editing. All authors have read and agreed to the published version of the manuscript.

Funding: The authors thank the "Faculdade de Ciências-UNESP-Bauru" for multi-user equipment (XRD). The authors thank the Brazilian agencies CNPq (grants #314.810/2021-8 and #421.677/2023-6), CAPES financial code 001, and FAPESP (grant #2024/01.1132-2) for their financial support.

Data Availability Statement: The original contributions presented in this study are included in the article. Further inquiries can be directed to the corresponding author.

Conflicts of Interest: The authors declare that they have no known competing financial interests.

References

1. Yang, Y.; Yan, S.; Qu, S.; Yi, M.; Chen, Z.; Zhou, T.; Xu, C. Microstructure of titanium alloy in additive/subtractive hybrid manufacturing: A review. *J. Alloys Compd.* **2025**, *1014*, 178769. [CrossRef]
2. Yadav, P.; Saxena, K.K. Effect of heat-treatment on microstructure and mechanical properties of Ti alloys: An overview. *Mater. Today Proc.* **2020**, *26*, 2546–2557. [CrossRef]
3. Lourenço, M.L.; Pontes, F.M.L.; Grandini, C.R. The Influence of Thermomechanical Treatments on the Structure, Microstructure, and Mechanical Properties of Ti-5Mn-Mo Alloys. *Metals* **2022**, *12*, 527. [CrossRef]
4. Sarma, J.; Kumar, R.; Sahoo, A.K.; Panda, A. Enhancement of material properties of titanium alloys through heat treatment process: A brief review. *Mater. Today Proc.* **2020**, *23*, 561–564. [CrossRef]
5. Gupta, J.; Jha, I.K.; Khatirkar, R.K.; Singh, J. Microstructure Evolution During Aging Heat Treatment of Metastable Ti-15V-3Cr-3Al-3Sn β Titanium Alloy. *J. Mater. Eng. Perform.* **2025**, *34*, 19945–19956. [CrossRef]
6. Xavier, C.C.; Correa, D.R.N.; Grandini, C.R.; Rocha, L.A. Low temperature heat treatments on Ti-15Zr-xMo alloys. *J. Alloys Compd.* **2017**, *727*, 246–253. [CrossRef]
7. Kuroda, P.A.B.; Quadros, F.d.F.; Afonso, C.R.M.; Grandini, C.R. The Effect of Solution Heat Treatment Time on the Phase Formation and Selected Mechanical Properties of Ti-25Ta-xZr Alloys for Application as Biomaterials. *J. Mater. Eng. Perform.* **2021**, *30*, 5905–5913. [CrossRef]
8. Lourenço, M.L.; Correa, M.R.; de Almeida, G.S.; Kuroda, P.A.B.; Zambuzzi, W.F.; Grandini, C.R. Development of new β Ti-10-Mo-Mn alloys for biomedical applications. *J. Alloys Compd.* **2024**, *1008*, 176524. [CrossRef]
9. Kuroda, P.A.B.; Carvalho, A.P.; Caram, R.; Figueiredo, R.B.; Afonso, C.R.M. Nanostructured bulk HPT β Ti-42Nb alloy as biomaterial for implants obtained directly from micrometric powders. *Mater. Lett.* **2025**, *378*, 137572. [CrossRef]
10. Correa, D.R.N.; Kuroda, P.A.B.; Grandini, C.R.; Rocha, L.A.; Oliveira, F.G.M.; Alves, A.C.; Toptan, F. Tribocorrosion behavior of β-type Ti-15Zr-based alloys. *Mater. Lett.* **2016**, *179*, 118–121. [CrossRef]
11. Kuroda, P.A.B.; Pedroso, B.L.T.; Pontes, F.M.L.; Grandini, C.R. Effect of Titanium Addition on the Structure, Microstructure, and Selected Mechanical Properties of As-Cast Zr-25Ta-xTi Alloys. *Metals* **2021**, *11*, 1507. [CrossRef]
12. de Mattos, F.; da Silva, A.; Sangali, M.; Rodrigues, J.; Caram, R.; Afonso, C. Unraveling composition graded microstructure of in-situ alloyed Ti-15Nb alloy through laser powder bed fusion. *Mater. Lett.* **2024**, *358*, 135776. [CrossRef]
13. Larson, A.C.; Dreele, R.B.V. *General Structure Analysis System (GSAS)*; Los Alamos National Laboratory Report LAUR; Los Alamos National Laboratory (LANL): Los Alamos, NM, USA, 2004.
14. Toby, B.H. R factors in Rietveld analysis: How good is good enough? *Powder Diffr.* **2012**, *21*, 67–70. [CrossRef]
15. Kuroda, P.A.B.; Grandini, C.R.; Afonso, C.R. Development of new β Ti and Zr-based alloys in the Ta-(75-x)Ti-xZr system. *J. Mater. Res. Technol.* **2024**, *29*, 4579–4587. [CrossRef]
16. *E92-16, A.D.*; Standard Test Methods for Vickers Hardness and Knoop Hardness of Metallic Materials. ASTM International: West Conshohocken, PA, USA, 2016.
17. *E384-16, A.D.*; Standard Test Method for Microindentation Hardness of Materials. ASTM International: West Conshohocken, PA, USA, 2016.
18. Rossi, M.C.; Bayerlein, D.L.; Gouvêa, E.d.S.; Haro Rodríguez, M.V.; Escuder, A.V.; Borrás, V.A. Evaluation of the influence of low Mg content on the mechanical and microstructural properties of β titanium alloy. *J. Mater. Res. Technol.* **2021**, *10*, 916–925. [CrossRef]
19. Elhadad, A.A.; Romero-Resendiz, L.; Rossi, M.C.; Rodríguez-Albelo, L.M.; Lascano, S.; Afonso, C.R.M.; Alcudia, A.; Amigó, V.; Torres, Y. Findings and perspectives of β-Ti alloys with biomedical applications: Exploring beyond biomechanical and biofunctional behaviour. *J. Mater. Res. Technol.* **2024**, *33*, 3550–3618. [CrossRef]
20. Cardoso, G.C.; de Almeida, G.S.; Corrêa, D.O.G.; Zambuzzi, W.F.; Buzalaf, M.A.R.; Correa, D.R.N.; Grandini, C.R. Preparation and characterization of novel as-cast Ti-Mo-Nb alloys for biomedical applications. *Sci. Rep.* **2022**, *12*, 11874. [CrossRef] [PubMed]
21. Martins Júnior, J.R.S.; Nogueira, R.A.; Araújo, R.O.d.; Donato, T.A.G.; Arana-Chavez, V.E.; Claro, A.P.R.A.; Moraes, J.C.S.; Buzalaf, M.A.R.; Grandini, C.R. Preparation and characterization of Ti-15Mo alloy used as biomaterial. *Mater. Res.* **2011**, *14*, 107–112. [CrossRef]
22. Hanada, S.; Izumi, O. Deformation and Fracture of Metastable Beta Titanium Alloys (Ti–15Mo–5Zr and Ti–15Mo–5Zr–3Al). *Trans. Jpn. Inst. Met.* **1982**, *23*, 85–94. [CrossRef]
23. Nunes, A.R.V.; Borborema, S.; Malet, L.; Dille, J.; de Almeida, L.H. Microstructural Evolution of Cold-Rolled β Metastable Ti-29Nb-2Mo-6Zr Alloy. *Microsc. Microanal.* **2019**, *25*, 2634–2635. [CrossRef]
24. Collings, E.W. *The Physical Metallurgy of Titanium Alloys*; ASM: Novelty, OH, USA, 1984.
25. Kuroda, P.A.B.; Quadros, F.d.F.; Araújo, R.O.d.; Afonso, C.R.M.; Grandini, C.R. Effect of Thermomechanical Treatments on the Phases, Microstructure, Microhardness and Young's Modulus of Ti-25Ta-Zr Alloys. *Materials* **2019**, *12*, 3210. [CrossRef] [PubMed]
26. Abbaschian, R.; Reed-Hill, R.E. *Physical Metallurgy Principles—SI Version*; Cengage Learning: Boston, MA, USA, 2009.

27. Callister, W.D., Jr.; Rethwisch, D.G. *Materials Science and Engineering: An Introduction*; John Wiley & Sons: Hoboken, NY, USA, 2020.
28. Kaur, M.; Singh, K. Review on titanium and titanium based alloys as biomaterials for orthopaedic applications. *Mater. Sci. Eng. C* **2019**, *102*, 844–862. [CrossRef] [PubMed]

Disclaimer/Publisher's Note: The statements, opinions and data contained in all publications are solely those of the individual author(s) and contributor(s) and not of MDPI and/or the editor(s). MDPI and/or the editor(s) disclaim responsibility for any injury to people or property resulting from any ideas, methods, instructions or products referred to in the content.